crystals

MDPI

Article

Structural Study of the Complex of *cblC* Methylmalonic Aciduria and Homocystinuria-Related Protein MMACHC with Cyanocobalamin

Qin Xu [1,2,3], Huan Zhou [1,2], Minjun Li [1,2], Weiwei Wang [1,2], Mengxue Xu [1], Zhimin Zhu [1,3], Chenyu Zhang [1,3], Qisheng Wang [1,2,*], Feng Yu [1,2,*] and Jianhua He [1,4,*]

1 Shanghai Institute of Applied Physics, Chinese Academy of Sciences, Shanghai 201800, China; xuqin@sinap.ac.cn (Q.X.); zhouhuan@sinap.ac.cn (H.Z.); liminjun@sinap.ac.cn (M.L.); wangww@sari.ac.cn (W.W.); 2018216024@njau.edu.cn (M.X.); zhuzhimin@sinap.ac.cn (Z.Z.); zhangchenyu@sinap.ac.cn (C.Z.)
2 Shanghai Synchrotron Radiation Facility, Shanghai Advanced Research Institute, Chinese Academy of Sciences, Shanghai 201204, China
3 University of Chinese Academy of Sciences, Beijing 100049, China
4 The Institute for Advanced Studies, Wuhan University, Wuhan 430072, China
* Correspondence: wangqisheng@sinap.ac.cn (Q.W.); yufeng@sinap.ac.cn (F.Y.); hejianhua@sinap.ac.cn (J.H.)

Abstract: MMACHC is an essential protein for the body to metabolise vitamin B_{12}, and its deficiency will cause *cblC*-type methylmalonic aciduria and homocystinuria. MMACHC can interact with cyanocobalamin (a type of vitamin B_{12}) cofactor and plays an important role in targeting cyanocobalamin to the enzyme of interest. In this paper, the GST-tag fusion-tagged MMACHC protein was successfully expressed by *Escherichia coli* (*E. coli*) low-temperature induction, and the high-purity MMACHC protein was successfully purified by affinity chromatography and gel filtration. Further, the crystal structure of MMACHC and cyanocobalamin complex was obtained with a resolution of 1.93 Å using X-ray diffraction. By analysing the complex structure of MMACHC and cyanocobalamin, we revealed the reasons for the diversity of MMACHC substrates and explained the reasons for the differences in disease conditions caused by different *MMACHC* site mutations. The acquisition of the complex structure of MMACHC and cyanocobalamin will play a significant role in promoting research on the metabolic pathway of vitamin B_{12}.

Keywords: MMACHC; cyanocobalamin; vitamin B_{12}; complex structure; X-ray diffraction

check for updates

Citation: Xu, Q.; Zhou, H.; Li, M.; Wang, W.; Xu, M.; Zhu, Z.; Zhang, C.; Wang, Q.; Yu, F.; He, J. Structural Study of the Complex of *cblC* Methylmalonic Aciduria and Homocystinuria-Related Protein MMACHC with Cyanocobalamin. *Crystals* **2022**, *12*, 468. https://doi.org/10.3390/cryst12040468

Academic Editor: Kil Sik Min

Received: 21 February 2022
Accepted: 16 March 2022
Published: 28 March 2022

Publisher's Note: MDPI stays neutral with regard to jurisdictional claims in published maps and institutional affiliations.

Copyright: © 2022 by the authors. Licensee MDPI, Basel, Switzerland. This article is an open access article distributed under the terms and conditions of the Creative Commons Attribution (CC BY) license (https://creativecommons.org/licenses/by/4.0/).

1. Introduction

Methylmalonic aciduria (MMA) is a heterogeneous autosomal recessive metabolic disorder of cobalamin (vitamin B_{12}) [1], which encompasses different complement groups, namely *cblA*–*cblG*, *cblJ*, *cblX*, and *mut* [2–5]. Cobalamin C (*cblC*) deficiency is the most common disorder and causes methylmalonic aciduria combined with homocystinuria. Previous studies suggested that homocysteine toxicity, glutathione metabolism, oxidative stress, the effects of the pharmacological activation, impaired methylation/phosphorylation, mislocalisation of RNA-binding proteins, and endoplasmic reticulum stress may contribute to disease onset [6–13].

The gene responsible for the *cblC* deficiency, which is called methylmalonic aciduria type C and homocystinuria (*MMACHC*), has been identified on chromosome 1p34.1 and catalyses the decyanation and dealkylation of cobalamin [14].

Vitamin B_{12} is a very large molecular organic compound, which can be called different cobalt amine according to the connection to a beta on cobalt different functional group (R group). In humans, there are two active cofactor forms of cobalamin, adenosylcobalamin (AdoCbl) for methylmalonyl CoA mutase and methylcobalamin (MeCbl) for methionine synthase (Figure 1). Although humans cannot synthesise cobalamin, we can ingest it from

the diet or receive it from gut bacteria [2]. However, as optical instability, the most incoming cobalamin from the diet is an inactive form—namely, cyanocobalamin (CNCbl). MMACHC catalyses CNCbl reductive decyanation to yield cob(II)alamin and cyanide. Cob(II)alamin can be converted to MeCbl or AdoCbl in the further reaction. Previous studies reported that MMACHC catalyses alkylcobalamins, such as MeCbl and AdoCbl, through a dealkylation reaction. This reaction may be involved in the regulation of MeCbl and AdoCbl in vivo [15].

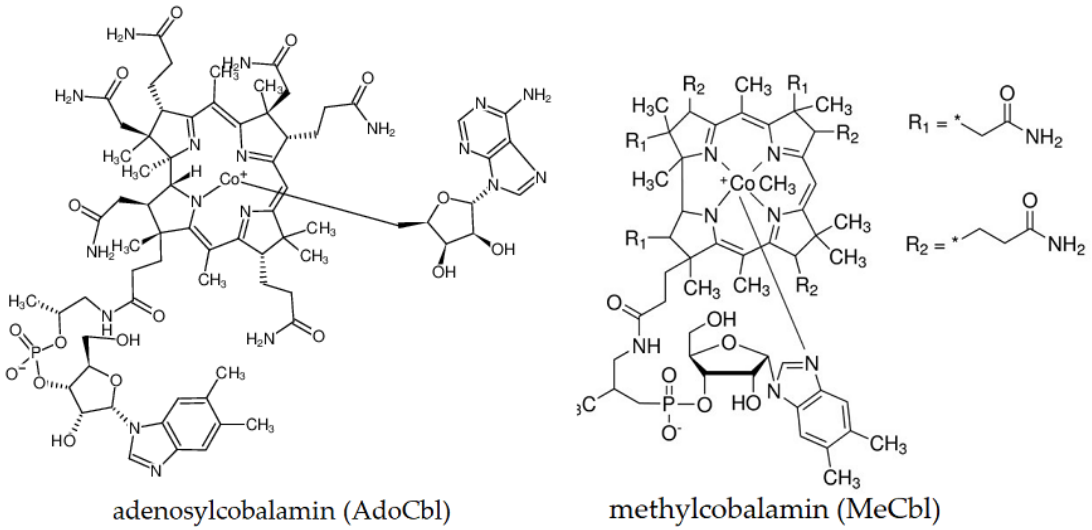


Figure 1. The structural formula of AdoCbl and MeCbl.

The full-length MMACHC contains 282 amino acids, and the mass weight is 31.7 kDa [14]. The primary sequence of MMACHC is well conserved among mammals, but no homologous proteins are known in prokaryotes. MMACHC includes an unconventional vitamin B_{12}-binding motif, and residues 122-HXXGX-126-154-GG-156 are important for vitamin B_{12} binding. Residues 181–282 in MMACHC display apparent structural similarity to the C-terminal domain (residues 152–239) of TonB protein, a domain that directly interacts with bacterial outer membrane receptors for import of vitamin B_{12} and iron-containing compounds [16]. Therefore, it was speculated that the C-terminal domain of MMACHC may also interact with the lysosomal transporter *LMBD1*, which helped vitamin B_{12} enter the cytoplasm [17]. Using surface plasmon resonance and bacterial two-hybrid system, it was confirmed that MMACHC can interact with methylmalonic aciduria and homocystinuria type D protein (MMADHC) [18].

Previous studies identified that MMACHC mutations are the cause of *cblC* deficiency [14,19]. *cblC* methylmalonic aciduria and homocystinuria caused by MMACHC mutations are the most common congenital defects in vitamin B_{12} metabolism [20]. That is because the metabolism of vitamin B_{12} has a significant relationship with the metabolism of homocysteine and folic acid [21]. For example, methionine synthetase requires mecobalamin as a coenzyme to catalyse the conversion of homocysteine from N^5-methyltetrahydrofolate to methionine. If *MMACHC* deficiency leads to mecobalamin deficiency, the synthesis of methionine is blocked, and excessive accumulation of homocysteine leads to homocystinuria. More critically, the regeneration of a tetrahydrofolic acid will be greatly affected, and tetrahydrofolic acid is a tool for methyl transport, which is required for the synthesis of both purine and pyrimidine. As a result, the nucleic acid synthesis disorder leads to abnormal cell division, which may eventually lead to megaloblastic anemia, also known as pernicious anemia [22].

There are two distinct *cblC* type defect phenotypes in terms of age of onset. Early-onset patients present with failure to thrive, megaloblastic anaemia, epilepsy, and neurodegenerative signs; late-onset patients present acute neurological symptoms after 4 years of age including spasticity, delirium, and psychosis. Pigmentary retinopathy with perimacular degeneration is part of the clinical disease manifestations [23,24]. Thus far, at least 60 dif-

ferent mutations in the *MMACHC* gene have been reported. Besides missense mutations, there are also many causing a putative premature truncation or deletion of the protein. The most common missense mutation is G147D [25,26], which is resulting in vitamin B_{12} unresponsive disease and early-onset disease. R161Q is the other common mutation that binds CNCbl with lower affinity than wild-type's and is associated with late-onset disease [25].

The mechanism of action of the decyanation and dealkylation processes of MMACHC is a very interesting question. It has been confirmed that the decyanation and dealkylation processes of MMACHC are carried out through two completely different chemical reactions [15,17]. In the presence of nicotinamide adenine dinucleotide phosphate (NADPH) and flavin adenine dinucleotide (FAD), CNCbl is converted to cyanide and CoB (II) Alamin through a reductant cyanidation process [17]. Alkylcobalamin requires nucleophilic substitution to produce CoB (I) Alamin in the presence of glutathione and then reoxidation to CoB (II) Alamin. At present, it has been confirmed that both MMACHC and C2–C6 alkylcobalamin have the ability to dealkylate [15]. Previous studies also reported that MMACHC was responsible for the early processing of both CNCbl (decyanation) and alkylcobalamins [27]. MMACHC does not belong to any known family of glutathione transferases, suggesting that MMACHC may represent a new class of glutathione transferases.

MMACHC is a 31.7 kDa protein [14], which may interact with LMBD1 and MMADMC and can decyanate and dealkylate in two completely different chemical reactions. Moreover, the substrate range is also quite wide and can help the structure transformation of cobalamin. This led to a great deal of interest in its protein structure. How does MMACHC contain so much functionality in such a small space?

2. Materials and Methods

2.1. Construction of MMACHC Expression Vector

The full-length *MMACHC* gene (residues 1–282, UniProt ID: Q9Y4U1) was cloned into plasmid pGEX-4T-1, which produces an N-terminally GST-tagged protein with a thrombin digestion site. Then, the MMACHC-pGEX-4T-1 expression plasmid was introduced into *E. coli* Rosetta(DE3)pLysS to express the recombinant *MMACHC*.

2.2. Overexpression and Purification of MMACHC

For overexpression of MMACHC, Rosetta(DE3)pLysS cells carrying the MMACHC expression vector were grown in LB medium with ampicillin at 37 °C. Isopropyl-1-thio-b-D-galactopyranoside (1 mM, final concentration) was added to the bacterial cultures (OD600 $\approx$ 0.8) to induce recombinant protein expression, and the cells were grown for 12 h with shaking at 16 °C. The bacterial pellet was resuspended in buffer A (140 mM NaCl, 2.7 mM KCl, 10 mM Na_2HPO_4, 1.8 mM KH_2PO_4, 5% glycerol, pH 7.3). Cells were lysed by passing through a microfluidiser (1250 bar; 1 bar = 100 kPa) three times; then, the lysate was centrifuged at 30,000$\times$ *g* for 30 min. The supernatant was loaded onto a 5 mL GSTrap column (GE Healthcare) that had been equilibrated in buffer A. After 20 column volumes of buffer A washing, GST-tagged MMACHC was eluted by using buffer B (20 mM Tris-HCl pH 8.0, 150 mM NaCl, 10 mM GSH, 5% glycerol). GST-tag was cut by using thrombin at 20 °C for 16 h and removed by GSTrap. MMACHC were loaded onto a Superdex 75 16/60 column that was equilibrated in buffer C (25 mM Tris-HCl pH 8.0, 150 mM NaCl, 5% glycerol). The resulting protein peak was concentrated to 15 mg/mL by using a 10 kDa MWCO Amicon Ultra and fresh TCEP was added to a final concentration of 2 mM. Aliquots were snap-frozen in liquid nitrogen and stored at −80 °C until they were used for crystallisation. Selenomethionine-labeled MMACHC (SeMet- MMACHC) protein was expressed in *E. coli* BL21 (DE3) cells using the M9 medium protocol. SeMet-MMACHC was expressed and purified using the same method as described for the wild-type MMACHC.

2.3. Crystallisation of MMACHC with CNCbl

Crystals of MMACHC with CNCbl were grown by hanging drop vapor diffusion at 18 °C. Equal volumes of 15 mg/mL protein were mixed with reservoir solution containing 25% PEG2000MME, 0.1 M Bis-Tris pH 6.5, 0.2 M Li_2SO_4.

2.4. Data Collection and Structure Determination

For the data collection, the crystals were soaked in a reservoir solution containing 20% glycerol and flash-cooled in liquid nitrogen. X-ray diffraction data were collected at beamline BL17U1 of Shanghai Synchrotron Radiation Facility (SSRF), People's Republic of China [28]. The Se-Met data were processed by using the HKL2000 software suite [29], and the initial SAD phase was solved by using SHELXC/D/E and hkl2map. The model was built using ARP/wARP and COOT [30] and then refined with Phenix [31–33]. The apo data were processed by using the xia2 software suite [34] and the molecular replacement method was carried out by using PHASER [35]. After molecular replacement, maximum-likelihood-based refinement of the atomic position, and temperature factors were performed with Phenix [31–33], and the atomic model was built with the program COOT [30]. Crystallographic statistics for the final models are shown in Table 1. Figures were prepared with PYMOL (http://www.pymol.org, 16 February 2022) [36].

Table 1. Data collection and refinement statistics.

	MMACHC with CNCbl
Data collection	
Space group	*C 1 2 1*
a, b, c (Å)	72.97 96.33 47.26
α, β, γ (°)	90.00 111.10 90.00
Wavelength (Å)	0.97915
Resolution (Å) [a]	55.6–1.93 (2.03–1.93)
$CC_{1/2}$ (a)	99.8 (99.8)
Unique reflections [a]	22,121
R_{meas} (%) [a]	4.8 (104)
Mean I/σ (I) [a]	11.8 (3.2)
Completeness (%) [a]	96.14 (96.81)
Multiplicity [a]	2.6 (2.6)
Refinement	
Resolution (Å)	33.37–1.93 (2.00–1.93)
R_{work}/R_{free} [b]	0.1602 (0.2020)
No.atoms	
Protein	1963
Ligand	108
Water	208
Average B factors (Å^2)	
Protein	28.02
Ligand	27.23
Water	28.9
RMS deviations	
Bond lengths (Å)	0.0163
Bond angles (°)	1.34
Ramachandran plot	
Favoured (%)	98.74
Allowed (%)	1.26
Outliers (%)	0

[a] The values in parentheses are for the outermost shell. [b] R_{free} is the R_{work} based on 5% of the data excluded from the refinement. $R_{meas} = \sum_{hkl} \sqrt{n/(n-1)} \sum_{i=1}^{n} \left| I_i(hkl) - \langle I(hkl) \rangle \right| / \sum_{hkl} \sum_i I_i(hkl)$, where $\langle I(hkl) \rangle$ is the mean intensity of a set of equivalent reflections. $R_{work} = \sum_{hkl} ||F_{obs}| - |F_{calc}|| / \sum_{hkl} |F_{obs}|$ where F_{obs} and F_{calc} are observed and calculated structure factors, respectively.

3. Results

3.1. MMACHC Purification and Gel-Filtration Chromatography

Using MMACHC-pGEX-4T-1 prokaryotic expression vector, MMACHC recombinant protein was successfully expressed in *E. coli* Rosetta(DE3)pLysS strain. After GST affinity chromatography purification, about 2 mg of MMACHC protein was obtained from 500 mL of culture medium. The MMACHC was then further purified by gel-filtration chromatography (Figure 2A). The apparent molecular weight of the protein was measured by gel-filtration chromatography and was about 45 kDa, which was slightly higher than theoretical molecular weight and SDS–PAGE results. The results of 15% SDS–PAGE showed that the protein purity reached more than 90%.

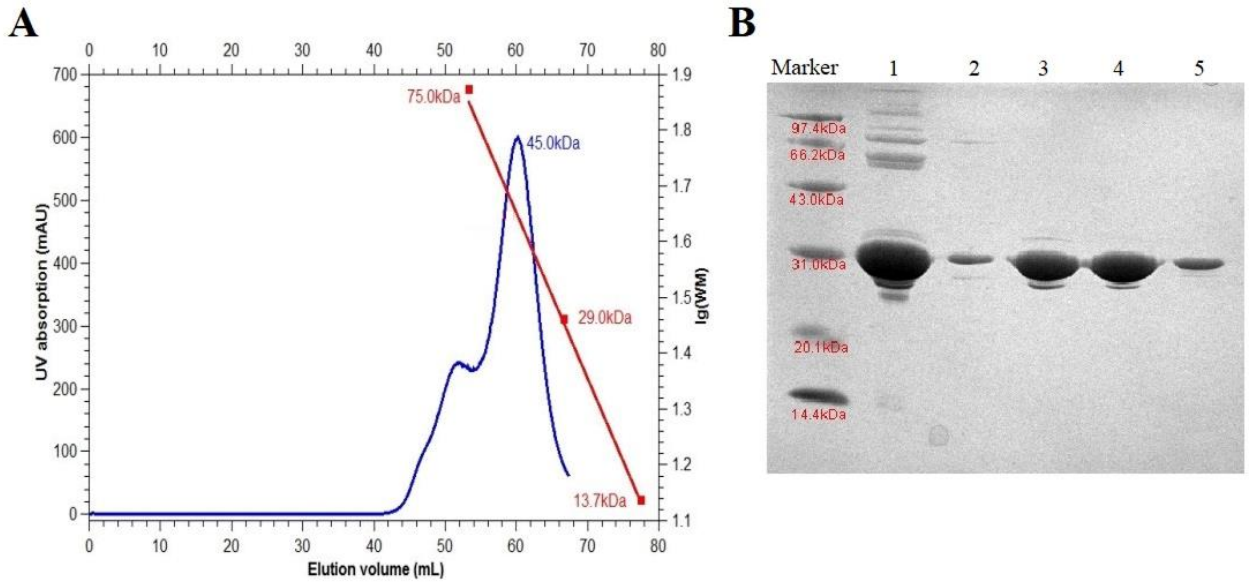


Figure 2. Protein purification of MMACHC: (**A**) Gel-filtration chromatography of MMACHC; (**B**) 15% SDS–PAGE analysis of recombinant MMACHC recovered from induced *Escherichia coli* cells. The SDS–PAGE was stained with Coomassie blue R-250. Lane M, molecular weight marker; lanes 1, purified recombinant MMACHC before gel filtration; lanes 2 to 5 denote further purified MMACHC by gel filtration.

3.2. Overall Structure of MMACHC with CNCbl

The MMACHC and CNCbl complex crystal (PDB code: 7WUZ) belonged to space group *C*2, with unit-cell parameters a = 72.97 Å, b = 96.33 Å, c = 47.26 Å, β = 111.10°. Detailed crystallographic data statistics for MMACHC and CNCbl complex structure are shown in Table 1. There were 287 residues in the asymmetric unit, including five residues introduced from the plasmid constructs, of which 241 residues can be matched to the electron density map.. The C terminus of MMACHC (242–282) was not observed (no clear electron density). The refined structure contained 2315 non-H protein atoms, 208 water molecules, 1 CNCbl molecule, 1 sulphate ion, and 1 tartrate ion (Figure 3A,B). Overall, 98.74% of all residues were located in the favoured region of the Ramachandran diagram. The R_{work} and R_{free} factors are 16.02% and 20.20%, respectively.

To investigate the conservation of MMACHC in eukaryotes, we extracted amino acids of MMACHC derived from different eukaryotes for multiple sequence alignment, which showed that MMACHC is relatively conserved in different eukaryotes, with three highly conserved amino acids (Figure 3C).

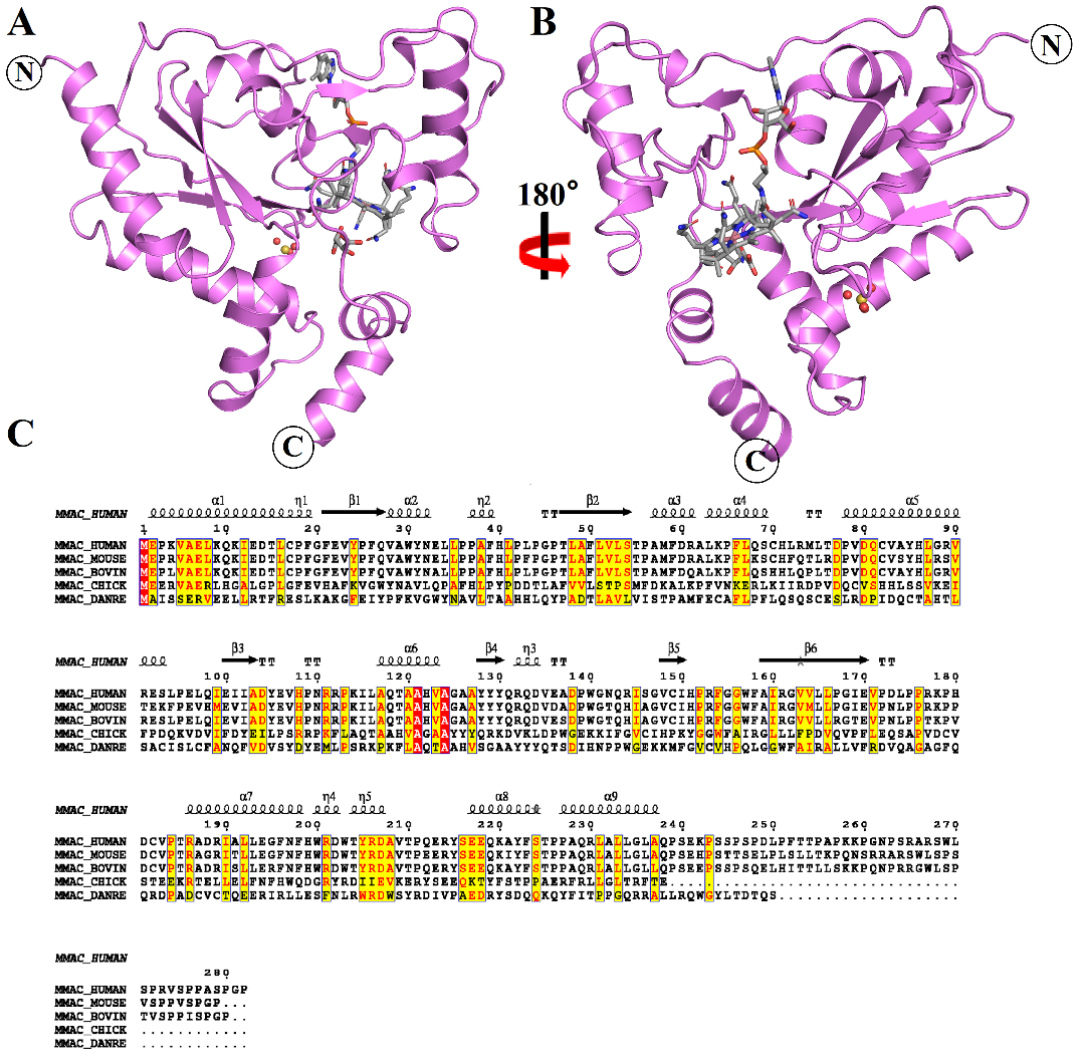


Figure 3. Structure overview of MMACHC with CNCbl: (**A**) crystal structure of the complex of MMACHC and CNCbl (MMACHC shown in violet and cartoon diagram, CNCbl shown in color and sticks); (**B**) the back view of crystal structure of the complex of MMACHC and CNCbl; (**C**) multiple sequence alignment results of MMACHC. The secondary structures of MMACHC are shown above. Red boxes indicate 100% homologous amino acids, while yellow boxes indicate 70% homologous amino acids. The protein names and UniProt codes are MMACHC from human (UniProt: Q9Y4U1); MMACHC from mouse (UniProt: Q9CZD0); MMACHC from bovine (UniProt: Q5E9C8); MMACHC from chick (UniProt: Q5ZL21); MMACHC from rat (UniProt: D4A729).

3.3. CNCbl Occupies the Ligand-Binding Site of MMACHC

To better determine the interaction of MMACHC with CNCbl and the presence of the MMACHC ligand-binding region, electron density maps of the ligand-binding sites were extracted from the overall electron density maps. Remarkably, a strip-shaped electron density map of CNCbl was found in the ligand-binding sites (consistent with the previous MMACHC and AdoCbl complex) (Figure 4), which also demonstrates the interaction of MMACHC with CNCbl and the presence of the MMACHC ligand-binding region.

3.4. Structural Comparison of MMACHC Combined with CNCbl and AdoCbl

To better clarify the difference between human MMACHC with CNCbl and AdoCbl (PDB code: 3SOM) [37], the structure of them was superposed (rmsd: 0.313, TM score: 0.6443). Comparing the two structures revealed that adenine was replaced by cyano in the MMACHC-CNCbl structure, and this cyano formed a certain spatial blockage that induced

a certain shift in MMACHC (Figure 5A). In order to verify the role of the cyano group, the structures of MMACHC with CNCbl and AdoCbl were further compared, and the results (Figure 5B,C) showed that the presence of the cyano group contributed to the instability of the α-helix and β-sheet of MMACHC (the part labelled by the rectangular box).

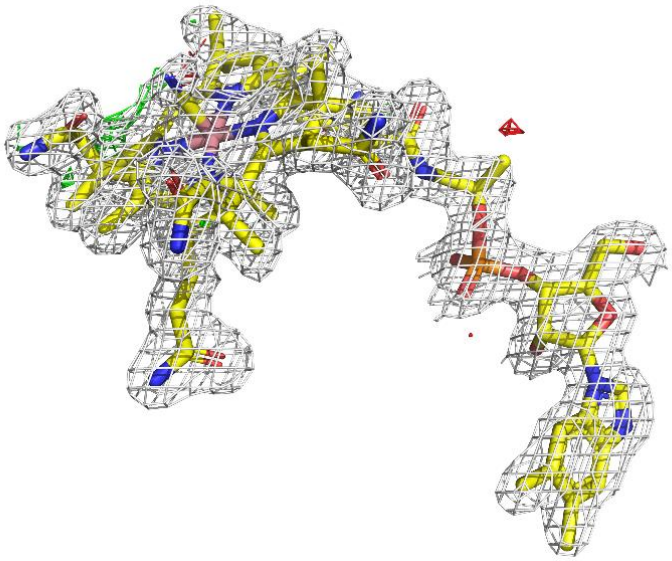


Figure 4. The electron density maps of CNCbl. $2F_o$–F_c (white) electron density maps were contoured at 1σ. F_o–F_c (red and green) electron density maps were contoured at −3σ and 3σ, respectively.

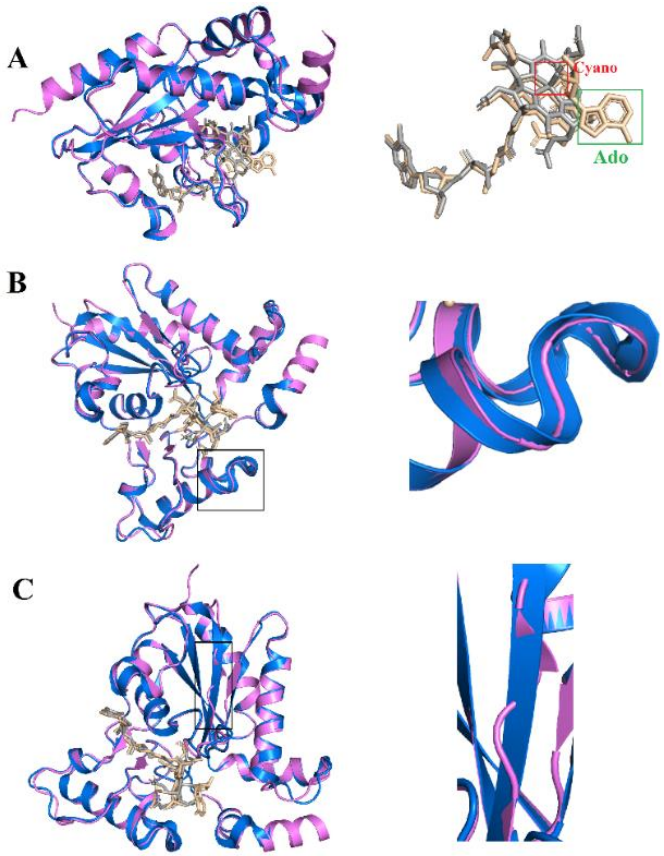


Figure 5. Structural comparison of *MMACHC* combined with CNCbl and AdoCbl, respectively: (**A**) structural comparison between two types cobalamin; (**B**) differences between *MMACHC* with CNCbl and AdoCbl on helix circled by black box; (**C**) differences between *MMACHC* with CNCbl and AdoCbl on β-sheet circled by black box.

4. Conclusions and Discussion

Methylmalonic aciduria combined with homocystinuria is a group of haematological and neurological disorders caused by congenital defects in the metabolism of vitamin B_{12}. The gene responsible for the *cblC* type of defect has been named methylmalonic aciduria type C and homocystinuria (MMACHC) [14]. The *cblC* type C methylmalonic aciduria combined with homocystinuria caused by the *MMACHC* mutations are the most common congenital defect in vitamin B_{12} metabolism and have the highest incidence.

Here, we well explained the substrate diversity of *MMACHC* and the different severity of symptoms caused by different mutation sites of *MMACHC* by resolving the structure of the *MMACHC* complex with CNCbl.

Firstly, there is a large space at the site where the cobalamin R group is located, large enough to hold a variety of different groups, such as methyl, hydroxyl, and adenosine, providing a structural basis for the substrate diversity of *MMACHC*.

Secondly, the severity of symptoms caused by different mutation sites in *MMACHC* varied. For example, patients with G147D mutation usually develop before one year of age, with symptoms such as dysplasia, seizures, lethargy and neurodegeneration, and even blood and eye abnormalities. This is because G147 is located in the region where *MMACHC* binds CNCbl, and the mutation disables *MMACHC*'s ability to bind CNCbl (Figure 6), so patients experience distress shortly after birth. In contrast, patients with R161Q mutation, which usually develops after the age of one and has symptoms such as dementia, behavioural problems, and myelopathy, have R161 located close to the location of the cyano and further away from the region that binds CNCbl, resulting in *MMACHC*-R161Q mutation having only one-fifth the ability to bind CNCbl of the wild type (Figure 6).

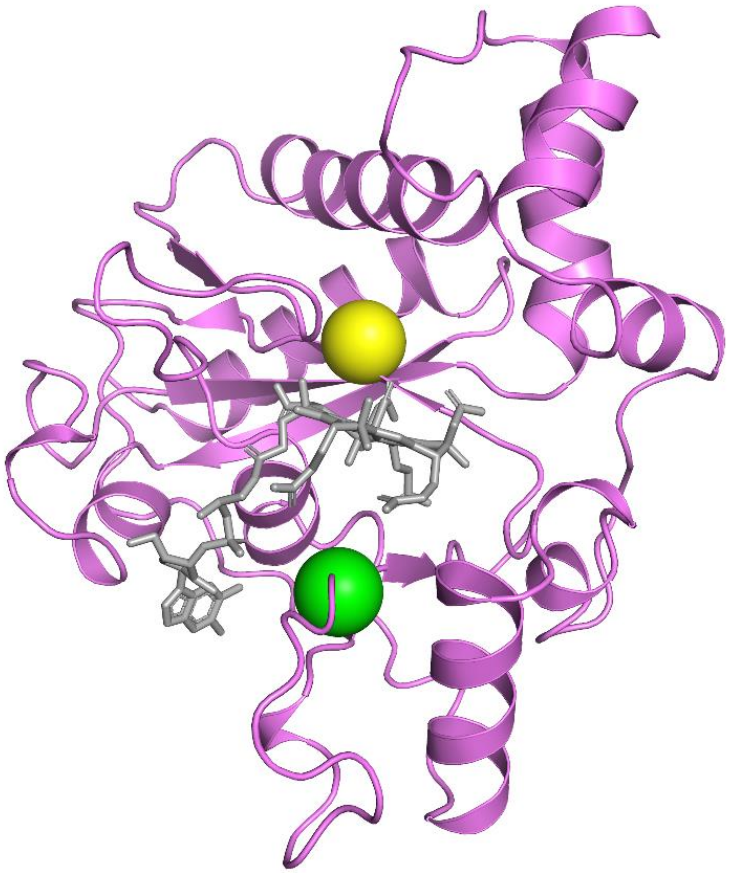


Figure 6. Crystal structure of the *MMACHC*-CNCbl complex, with the yellow ball at R161 and the green ball at G147.

The structures shown by these two groups are quite consistent with the structures resolved in this study. The determination of the crystal structure of the *MMACHC* and cyanocobalamin complexes contributes to a better understanding of the metabolic pathways of vitamin B_{12}.

Author Contributions: Data curation, Q.X.; Formal analysis, H.Z., M.L., W.W., M.X., Z.Z., C.Z. and F.Y.; Funding acquisition, Q.W., J.H. and F.Y.; Investigation, J.H.; Software, F.Y.; Supervision, Q.W. and J.H.; Validation, Q.X. and F.Y.; Visualization, F.Y.; Writing—original draft, Q.X., H.Z., M.L., W.W., M.X., Z.Z. and C.Z.; Writing—review & editing, Q.X., Q.W., F.Y. and J.H. All authors have read and agreed to the published version of the manuscript.

Funding: This research was funded by The National Key Research and Development Program of China, grant number 2017YFA0504901, and The National Natural Science Foundation Grants of China grant number 31100529.

Acknowledgments: The authors thank the teams at the BL17U1 beamline of the Shanghai Synchrotron Radiation Facility for the beamtime and the User Experiment Assist System of SSRF allocated to this project and for their help in experiments.

Conflicts of Interest: The authors declare no conflict of interest.

References

1. Rosenblatt, D.S.; Cooper, B.A. Inherited disorders of vitamin B_{12} metabolism. *Blood Rev.* **1987**, *1*, 177–182. [CrossRef]
2. Quadros, E.V. Advances in the understanding of cobalamin assimilation and metabolism. *Br. J. Haematol.* **2010**, *148*, 195–204. [CrossRef] [PubMed]
3. Jones, P.; Patel, K.; Rakheja, D. Chapter 9—Disorder: Methylmalonic aciduria. In *A Quick Guide to Metabolic Disease Testing Interpretation*, 2nd ed.; Jones, P., Patel, K., Rakheja, D., Eds.; Academic Press: Cambridge, MA, USA, 2020; pp. 51–56. [CrossRef]
4. Watkins, D.; Venditti, C.P.; Rosenblatt, D.S. Chapter 51—Vitamins: Cobalamin and folate. In *Rosenberg's Molecular and Genetic Basis of Neurological and Psychiatric Disease*, 2nd ed.; Rosenberg, R.N., Pascual, J.M., Eds.; Academic Press: Cambridge, MA, USA, 2020; pp. 687–697. [CrossRef]
5. Watkins, D.; Venditti, C.P.; Rosenblatt, D.S. Chapter 47—Vitamins: Cobalamin and Folate. In *Rosenberg's Molecular and Genetic Basis of Neurological and Psychiatric Disease*, 5th ed.; Rosenberg, R.N., Pascual, J.M., Eds.; Academic Press: Boston, MA, USA, 2015; pp. 521–529. [CrossRef]
6. Guire, P.; Parikh, A.; Diaz, G.A. Profiling of oxidative stress in patients with inborn errors of metabolism. *Mol. Genet. Metab.* **2009**, *98*, 173–180. [CrossRef] [PubMed]
7. Richard, E.; Jorge-Finnigan, A.; Garcia-Villoria, J.; Merinero, B.; Pineda, M. Genetic and cellular studies of oxidative stress in methylmalonic aciduria (MMA) cobalamin deficiency type C (cblC) with homocystinuria (MMACHC). *Hum. Mutat.* **2010**, *30*, 1558–1566. [CrossRef] [PubMed]
8. Caterino, M.; Pastore, A.; Strozziero, M.G.; Giovamberardino, G.D.; Imperlini, E.; Scolamiero, E.; Ingenito, L.; Boenzi, S.; Ceravolo, F.; Martinelli, D. The proteome of cblC defect: In vivo elucidation of altered cellular pathways in humans. *J. Inherit. Metab. Dis.* **2015**, *38*, 969–979. [CrossRef] [PubMed]
9. Hannibal, L.; Dibello, P.M.; Yu, M.; Miller, A.; Wang, S.; Willard, B.; Rosenblatt, D.S.; Jacobsen, D.W. The MMACHC proteome: Hallmarks of functional cobalamin deficiency in humans. *Mol. Genet. Metab.* **2011**, *103*, 226–239. [CrossRef] [PubMed]
10. Pastore, A.; Martinelli, D.; Piemonte, F.; Tozzi, G.; Dionisi-Vici, C. Glutathione metabolism in cobalamin deficiency type C (cblC). *J. Inherit. Metab. Dis.* **2013**, *37*, 125–129. [CrossRef]
11. Battaglia-Hsu, S.-F.; Ghemrawi, R.; Coelho, D.; Dreumont, N.; Mosca, P.; Hergalant, S.; Gauchotte, G.; Sequeira, J.M.; Ndiongue, M.; Houlgatte, R.; et al. Inherited disorders of cobalamin metabolism disrupt nucleocytoplasmic transport of mRNA through impaired methylation/phosphorylation of ELAVL1/HuR. *Nucleic Acids Res.* **2018**, *46*, 7844–7857. [CrossRef]
12. Rashka, C.; Hergalant, S.; Dreumont, N.; Oussalah, A.; Coelho, D. Analysis of fibroblasts from patients with cblC and cblG genetic defects of cobalamin metabolism reveals global dysregulation of alternative splicing. *Hum. Mol. Genet.* **2020**, *29*, 1969–1985. [CrossRef]
13. Ghemrawi, R.; Arnold, C.; Battaglia-Hsu, S.-F.; Pourié, G.; Trinh, I.; Bassila, C.; Rashka, C.; Wiedemann, A.; Flayac, J.; Robert, A.; et al. SIRT1 activation rescues the mislocalization of RNA-binding proteins and cognitive defects induced by inherited cobalamin disorders. *Metabolism* **2019**, *101*, 153992. [CrossRef]
14. Lerner-Ellis, J.P.; Tirone, J.C.; Pawelek, P.D.; Doré, C.; Atkinson, J.L.; Watkins, D.; Morel, C.F.; Fujiwara, T.M.; Moras, E.; Hosack, A.R.; et al. Identification of the gene responsible for methylmalonic aciduria and homocystinuria, cblC type. *Nat. Genet.* **2006**, *38*, 93–100. [CrossRef] [PubMed]
15. Kim, J.; Hannibal, L.; Gherasim, C.; Jacobsen, D.W.; Banerjee, R. A Human Vitamin B_{12} Trafficking Protein Uses Glutathione Transferase Activity for Processing Alkylcobalamins. *J. Biol. Chem.* **2009**, *284*, 33418–33424. [CrossRef] [PubMed]

16. Pawelek, P.D.; Croteau, N.; Ng-Thow-Hing, C.; Khursigara, C.M.; Moiseeva, N.; Allaire, M.; Coulton, J.W. Structure of TonB in Complex with FhuA, E. coli Outer Membrane Receptor. *Science* **2006**, *312*, 1399–1402. [CrossRef] [PubMed]
17. Kim, J.; Gherasim, C.; Banerjee, R. Decyanation of vitamin B_{12} by a trafficking chaperone. *Proc. Natl. Acad. Sci. USA* **2008**, *105*, 14551–14554. [CrossRef] [PubMed]
18. Plesa, M.; Kim, J.; Paquette, S.G.; Gagnon, H.; Ng-Thow-Hing, C.; Gibbs, B.F.; Hancock, M.A.; Rosenblatt, D.S.; Coulton, J.W. Interaction between MMACHC and MMADHC, two human proteins participating in intracellular vitamin B_{12} metabolism. *Mol. Genet. Metab.* **2011**, *102*, 139–148. [CrossRef]
19. Lerner-Ellis, J.P.; Anastasio, N.; Liu, J.; Coelho, D.; Suormala, T.; Stucki, M.; Loewy, A.D.; Gurd, S.; Grundberg, E.; Morel, C.F.; et al. Spectrum of mutations in MMACHC, allelic expression, and evidence for genotype–phenotype correlations. *Hum. Mutat.* **2009**, *30*, 1072–1081. [CrossRef]
20. Chang, J.-T.; Chen, Y.-Y.; Liu, T.-T.; Liu, M.-Y.; Chiu, P.-C. Combined Methylmalonic Aciduria and Homocystinuria cblC Type of a Taiwanese Infant With c.609G>A and c.567dupT Mutations in the MMACHC Gene. *Pediatrics Neonatol.* **2011**, *52*, 223–226. [CrossRef]
21. Watkins, D.; Rosenblatt, D.S. Lessons in biology from patients with inborn errors of vitamin B12 metabolism. *Biochimie* **2013**, *95*, 1019–1022. [CrossRef]
22. Martinelli, D.; Deodato, F.; Dionisi-Vici, C. Cobalamin C defect: Natural history, pathophysiology, and treatment. *J. Inherit. Metab. Dis.* **2011**, *34*, 127–135. [CrossRef]
23. Rosenblatt, D.S.; Aspler, A.L.; Shevell, M.I.; Pletcher, B.A.; Fenton, W.A.; Seashore, M.R. Clinical heterogeneity and prognosis in combined methylmalonic aciduria and homocystinuria (cblC). *J. Inherit. Metab. Dis.* **1997**, *20*, 528–538. [CrossRef]
24. Rossi, A.; Cerone, R.; Biancheri, R.; Gatti, R.; Tortori-Donati, P. Early-onset combined methylmalonic aciduria and homocystinuria: Neuroradiologic findings. *Ajnr Am. J. Neuroradiol.* **2001**, *22*, 554–563. [CrossRef] [PubMed]
25. Froese, D.S.; Healy, S.; McDonald, M.; Kochan, G.; Oppermann, U.; Niesen, F.H.; Gravel, R.A. Thermolability of mutant MMACHC protein in the vitamin B_{12}-responsive cblC disorder. *Mol. Genet. Metab.* **2010**, *100*, 29–36. [CrossRef] [PubMed]
26. Froese, D.S.; Zhang, J.; Healy, S.; Gravel, R.A. Mechanism of vitamin B_{12}-responsiveness in cblC methylmalonic aciduria with homocystinuria. *Mol. Genet. Metab.* **2009**, *98*, 338–343. [CrossRef] [PubMed]
27. Hannibal, L.; Kim, J.; Brasch, N.E.; Wang, S.; Rosenblatt, D.S.; Banerjee, R.; Jacobsen, D.W. Processing of alkylcobalamins in mammalian cells: A role for the MMACHC (cblC) gene product. *Mol. Genet. Metab.* **2009**, *97*, 260–266. [CrossRef]
28. Wang, Q.-S.; Zhang, K.-H.; Cui, Y.; Wang, Z.-J.; Pan, Q.-Y.; Liu, K.; Sun, B.; Zhou, H.; Li, M.-J.; Xu, Q.; et al. Upgrade of macromolecular crystallography beamline BL17U1 at SSRF. *Nucl. Sci. Tech.* **2018**, *29*, 68. [CrossRef]
29. Otwinowski, Z.; Minor, W. Processing of X-Ray Diffraction Data Collected in Oscillation Mode. *Methods Enzymol.* **1997**, *276*, 276307–276326. [CrossRef]
30. Emsley, P.; Cowtan, K. Coot: Model-building tools for molecular graphics. *Acta Crystallogr. Sect. D Biol. Crystallogr.* **2004**, *60*, 2126–2132. [CrossRef]
31. Adams, P.D.; Grosse-Kunstleve, R.W.; Li, W.H.; Ioerger, T.R.; Terwilliger, T.C. PHENIX: Building new software for automated crystallographic structure determination. *Acta Crystallogr. Sect. D Biol. Crystallogr.* **2002**, *58*, 1948–1954. [CrossRef]
32. Afonine, P.V.; Grosse-Kunstleve, R.W.; Echols, N.; Headd, J.J.; Moriarty, N.W.; Mustyakimov, M. Towards automated crystallographic structure refinement with phenix.refine. *Acta Crystallogr. Sect. D. Biol. Crystallogr.* **2012**, *68*, 352–367. [CrossRef]
33. Adams, P.D.; Afonine, P.V.; Bunkoczi, G.; Chen, V.B.; Davis, I.W.; Echols, N.; Headd, J.J.; Hung, L.-W.; Kapral, G.J.; Grosse-Kunstleve, R.W.; et al. PHENIX: A comprehensive Python-based system for macromolecular structure solution. *Acta Crystallogr. Sect. D* **2010**, *66*, 213–221. [CrossRef]
34. Graeme, W.; Lobley, C.; Prince, S.M. Decision making in xia2. *Acta Crystallogr. Sect. D Biol. Crystallogr.* **2018**, *69*, 1260–1273. [CrossRef]
35. Mccoy, A.J.; Grosse-Kunstleve, R.W.; Adams, P.D.; Winn, M.D.; Storoni, L.C.; Read, R.J. Phaser crystallographic software. *J. Appl. Crystallogr.* **2007**, *40*, 658–674. [CrossRef] [PubMed]
36. Delano, W.L. The PyMol Molecular Graphics System. *Proteins Struct. Funct. Bioinform.* **2002**, *30*, 442–454.
37. Froese, D.S.; Krojer, T.; Wu, X.; Shrestha, R.; Kiyani, W.; Delft, F.V.; Gravel, R.A.; Oppermann, U.; Yue, W.W. Structure of MMACHC Reveals an Arginine-Rich Pocket and a Domain-Swapped Dimer for Its B_{12} Processing Function. *Biochemistry* **2012**, *51*, 5083–5090. [CrossRef]